

EEEN 415: Assignment 1

H. S. Chin; 300493343

21rd of August 2022

Section A - Formative Questions

Sketch Nyquist plot (or use Matlab) and use the diagram to assess the stability of the following transfer functions. Consider whether each system is stable as written, and whether it could be driven into either instability or stability by increasing or decreasing the gain sufficiently. For unstable systems, describe how many poles would be in the right half of the s-plane for the closed loop system and sketch their response (you can use Matlab to confirm your result here, but you should make sure you can do this instability prediction manually).

- **RHS:** right hand side of the s plane

1a

$$\begin{aligned} G_1(s) &= \frac{20(s^2 + s + 0.5)}{s(s+1)(s+10)} \\ &= \frac{20s^2 + 20s + 10}{s^3 + 11s^2 + 10s} \end{aligned}$$

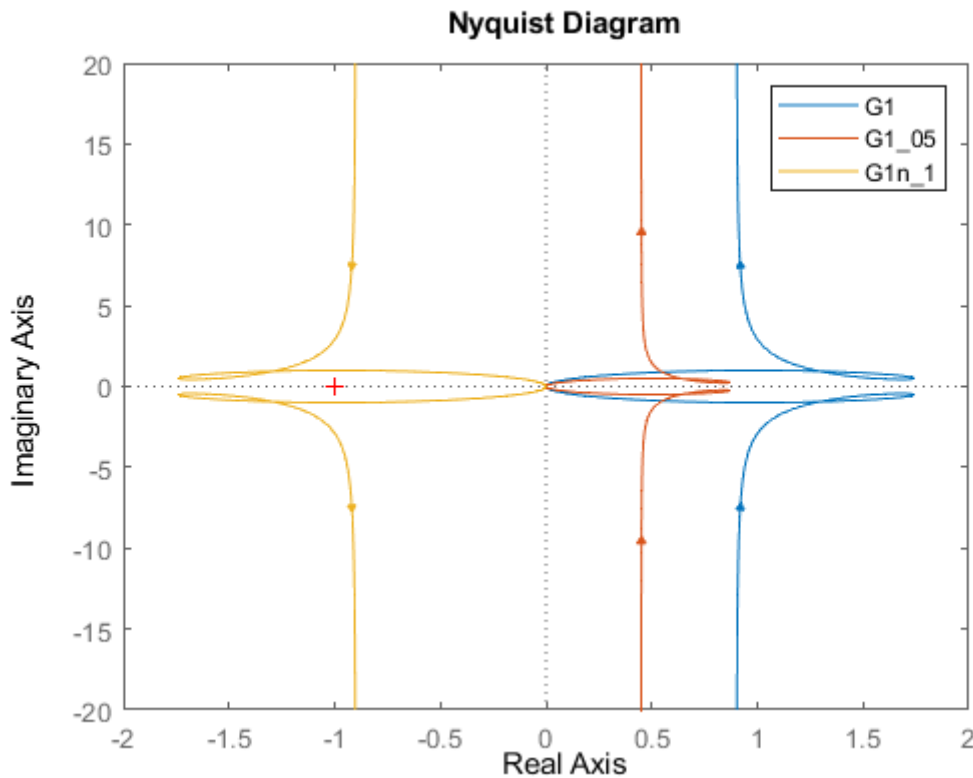


Figure 1: $G_1(s)$ Nyquist plots.

As there is no RHS pole in $G_1(s)$'s open loop TF and the Nyquist contour does not have any clockwise encirclement of the critical point, the closed loop system is stable. Additionally, the closed loop system is stable for all gains between $-\infty$ and $+\infty$ as illustrated in all the Nyquist contours of Figure 1.

$$\left\{ \begin{array}{l} \text{stable} \end{array} \right. \quad -\infty < g \leq \infty$$

1b

$$\begin{aligned}
 G_2(s) &= \frac{s^2 + 3}{(s + 1)^2} \\
 &= \frac{s^2 + 3}{s^2 + 2s + 1}
 \end{aligned}$$

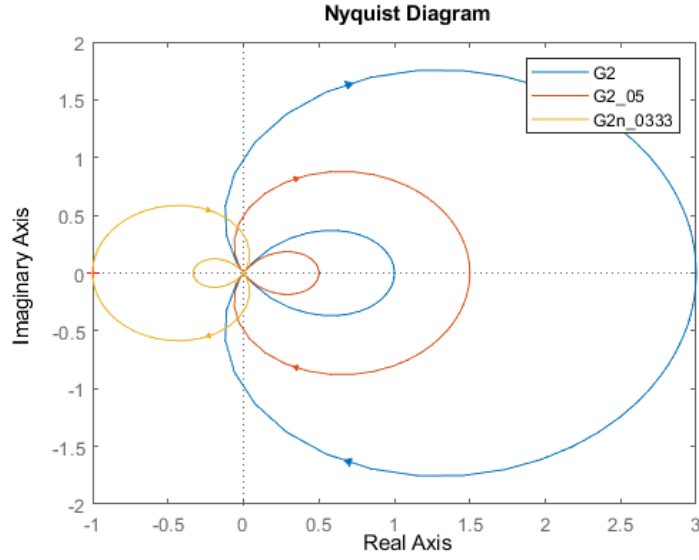


Figure 2: $G_2(s)$ Nyquist plots.

As there is no RHS pole in $G_2(s)$'s open loop TF, and the Nyquist contours does not have any clockwise encirclement of the critical point. The closed loop system will be stable. However, the system will become marginally stable at a gain of -0.333 , and any gain less than -0.333 will become unstable as shown in Figure 2's brown and yellow Nyquist contours.

$$\begin{cases}
 \text{unstable} & g < -0.333 \\
 \text{marginally stable} & g = -0.333 \\
 \text{stable} & -0.333 < g \leq \infty
 \end{cases}$$

1c

$$G_3(s) = \frac{1000}{s(s+1)(s+20)}$$

$$= \frac{1000}{s^3 + 21s^2 + 20s}$$

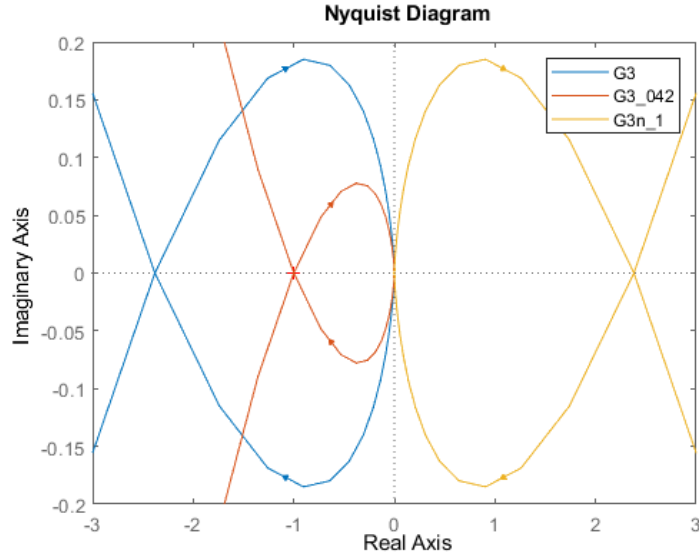


Figure 3: $G_3(s)$ Nyquist plots zoom out.

Although there is no RHS pole in $G_3(s)$'s open loop TF, the Nyquist contour does have at least one clockwise encirclement of the critical point, thus, the closed loop system will be unstable. Although it may look like the critical point was encircled once, the contour must meet again, hence creating 2 encirclements around the critical point. (example can be seen in Figure 4). However, with little gain or negative gain, the closed system will become stable as shown in the brown and yellow contours of Figure 3.

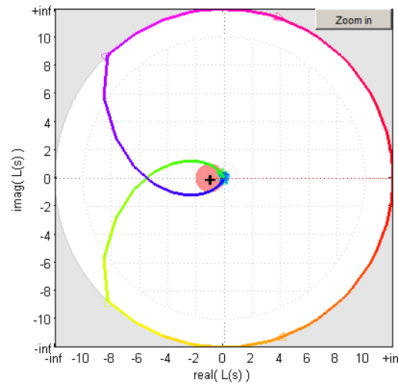


Figure 4: $G_3(s)$ expected zoom out of G_3 .

$$\begin{cases} \text{stable} & g < 0.42 \\ \text{unstable} & g > 0.42 \end{cases}$$

1d

$$\begin{aligned}
 G_4(s) &= \frac{-1000}{(s-1)(s+1)(s+20)} \\
 &= \frac{-1000}{s^3 + 20s^2 - s - 20} \\
 s &= -20.0993, 0.0496 \pm 0.9963i
 \end{aligned}$$

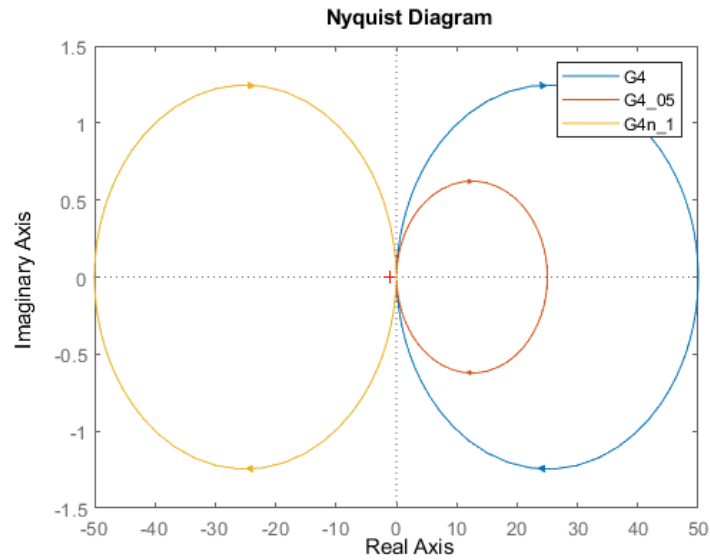


Figure 5: $G_4(s)$ Nyquist plot.

Although the Nyquist contour does not encircle the critical point, there are 2 RHS poles in $G_4(s)$'s open loop TF, thus, the closed loop system will be unstable. Additionally, any negative gain will result in a clockwise encirclement of the critical point resulting in an unstable closed loop system.

2

Consider a system that has a complex pair of poles in the s-plane that correspond to a mode having a damped frequency of 1 krad/s and a damping ratio of 0.1. Find the equivalent locations in the z-plane using a sampling frequency that puts the Nyquist frequency ten times higher than pole location (ie 10 krad/s), as well as a sampling frequency that is only 3 times higher.

For each sampling frequency plot the impulse response, the bode plot and the root locus diagram of the discrete time system. Comment on the differences between the results obtained from the two sampling rates, as well as how well they approximate the continuous time system.

s plane pole location:

$$\begin{aligned}
 \zeta &= 0.1 \\
 \omega_d &= 1 \text{krad/s} \\
 \omega_n &= \frac{\omega_d}{\sqrt{1 - \zeta^2}} \\
 &= 1.005 \text{krad/s} \\
 &= 1005 \text{rad/s} \\
 \lambda_s &= -\zeta\omega_n \pm j\omega_n\sqrt{1 - \zeta^2} \\
 &= -0.1 * 1005 \pm j\omega_n\sqrt{1 - 0.1^2} \\
 &= -100.5 \pm 1000j
 \end{aligned}$$

z plane pole location:

$$\begin{aligned}
 t_s &= \frac{\pi}{\omega_{max}} \\
 \omega_{max} &= 10 \text{krad/s}, 3 \text{krad/s} \\
 t_{s(10 \text{krad/s}, 3 \text{krad/s})} &= 0.000314, 0.001047 \\
 \lambda_z &= e^{\lambda_s t_s} \\
 &= e^{-\zeta\omega_n t_s} \angle \pm \omega_d t_s \\
 &= e^{-0.1 * 1005 * t_s} \angle \pm 1000 * t_s \\
 \lambda_{z10 \text{krad/s}} &= 0.9689 \angle \pm 0.3142 \\
 \lambda_{z3 \text{krad/s}} &= 0.9001 \angle \pm 1.0472
 \end{aligned}$$

pole locations at the given sampling rate can be shown in rectangular form below.

$$\begin{aligned}
 P_{z(10 \text{krad/s})} &= [0.9215 \pm 0.2994j] \\
 P_{z(3 \text{krad/s})} &= [0.4500 + 0.7795j]
 \end{aligned}$$

z-plane poles associated with 10 krad/s.

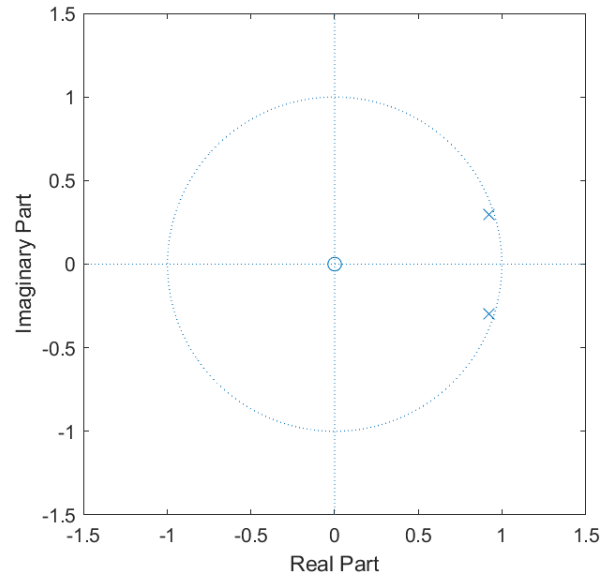


Figure 6: z-plane poles of $t_s = 10$.

z-plane poles associated with 3 krad/s.

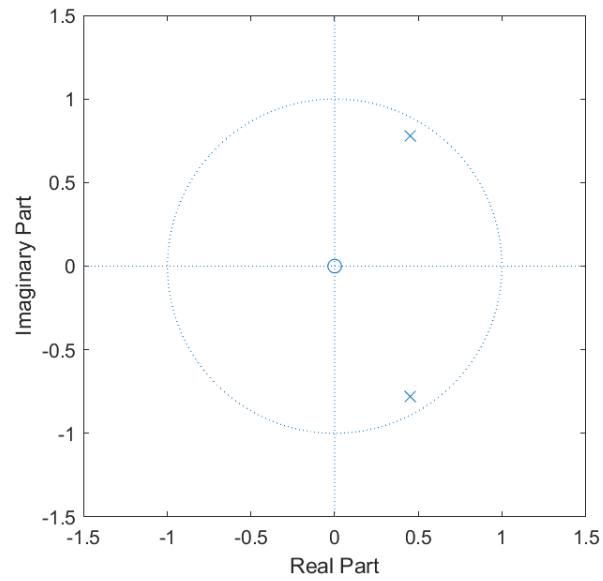


Figure 7: z-plane poles of $t_s = 3$.

step response associated with $t_s = 10$ (blue) $t_s = 3$ (orange).

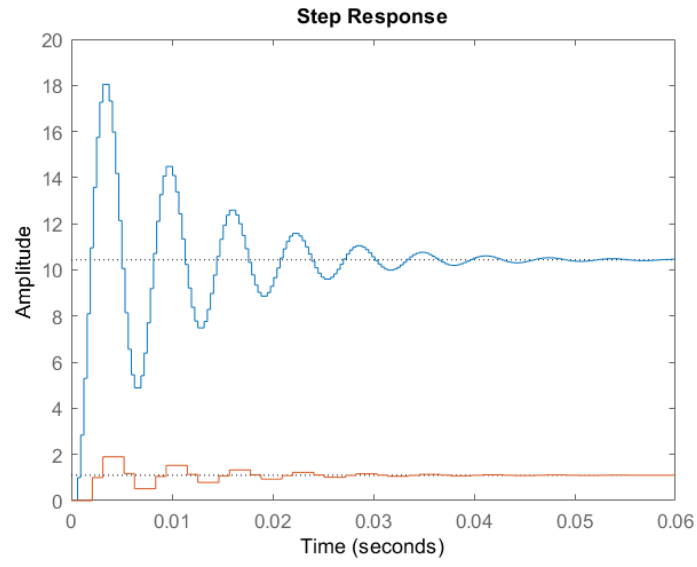


Figure 8: step responses of $t_s = 10, 3$.

bode plots associated with $t_s = 10$ (blue) $t_s = 3$ (orange).

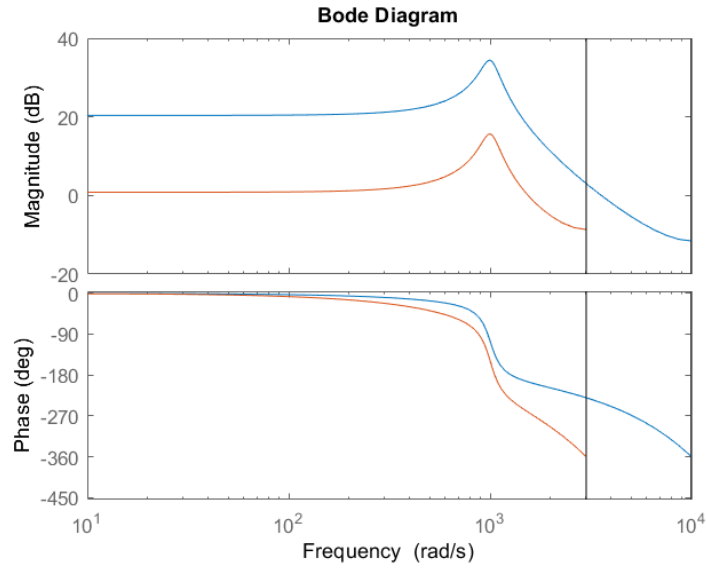


Figure 9: bode plots of $t_s = 10, 3$.

root locus associated with $t_s = 10$ (blue) $t_s = 3$ (orange).

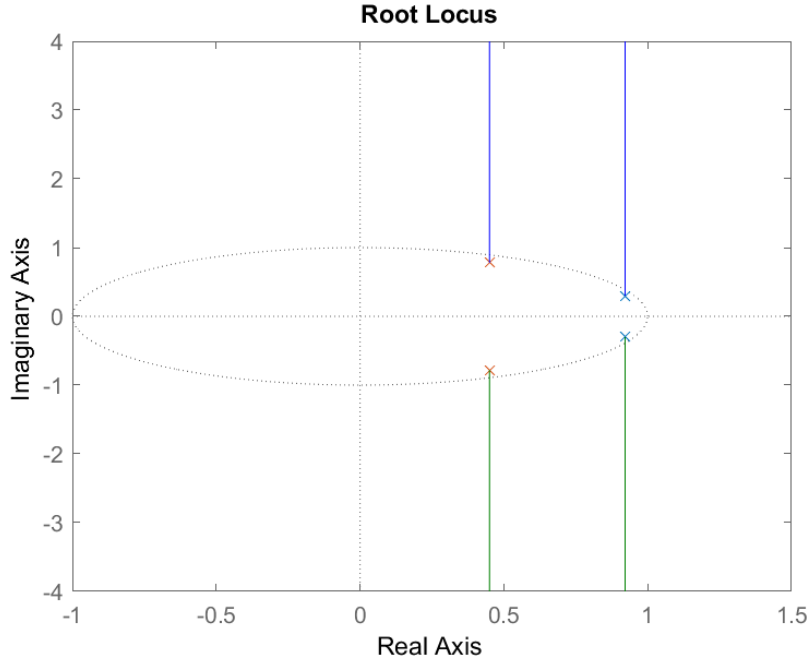


Figure 10: root locus of $t_s = 10, 3$.

As observed in Figures above, the varying damped frequencies was placed in line with $\zeta = 0.1$, in accordance with the damping ratio, at different frequencies. Consequently, when we increase the sampling rate from $t_s = 3$ to $t_s = 10$ the oscillation was enlarged, as illustrated in Figure 8. This was expected as greater sampling rates produce an approximation closer to the continuous time system.

Section B - Summative Questions

The dynamics of the simple boom crane discussed in lectures are governed by a set of differential equations, where the various variables are as defined in the lecture notes. However, rather than starting with these differential equations, we will use simplified transfer functions that describe how the two inputs (boom torque and winch torque) produce changes in the two output variables (the x and y positions of the load).

A transfer function model necessarily omits the nonlinear effects that the real crane would exhibit. We will return to look at a higher fidelity model later in the course, where we will be able to see the nonlinear properties of the system.

The transfer function between winch torque and the y-position of the load is

$$\frac{Y(s)}{\theta_w(s)} = \frac{10}{s^2 + \frac{b_1}{m}s + \frac{k_1}{m}s}$$

We will assume that the winch torque produces no motion of the load in the x-direction, so the transfer function between winch torque and the x-position of the load is

$$\frac{X(s)}{\theta_w(s)} = 0$$

The position change of the boom is coupled into changes in both the x and y positions of the load.

$$\begin{aligned}\frac{Y(s)}{\theta_b(s)} &= -\frac{\sqrt{2}}{s^2 + \frac{b_b}{M}s + \frac{k_b}{M}} \\ \frac{X(s)}{\theta_b(s)} &= -\frac{\sqrt{2}\frac{g}{l_p}}{(s^2 + \frac{b_b}{M}s + \frac{k_b}{M})(s^2 + \frac{b_b}{l_p}s + \frac{g}{l_p})}\end{aligned}$$

Objective

- Devise a closed loop control system for the boom and the winch to dampen the motion of the load in both x and y direction.
- Assume that the load begins with an initial x-location of 10° (remove it).
- Motion in the x direction must not oscillate more than 0.2 m after 5 s.
- Motion in the y direction must not oscillate more than 0.1 m after 5 s.

$$\begin{aligned}\frac{Y(s)}{\theta_w(s)} &= \frac{10}{s^2 + 3s + \frac{s}{10}} \\ \frac{Y(s)}{\theta_b(s)} &= \frac{-\sqrt{2}}{s^2 + \frac{3s}{4} + 25} \\ \frac{X(s)}{\theta_b(s)} &= \frac{-\sqrt{2}\frac{9.81}{2}}{s^4 + \frac{4s^3}{5} + 29.94s^2 + 4.925s + 122.5}\end{aligned}$$

Using the provided physical parameters, the transfer functions for the winch and the boom can be simplified as shown above.

Design a x-controller that acts on the boom to affect the x-position of the load.

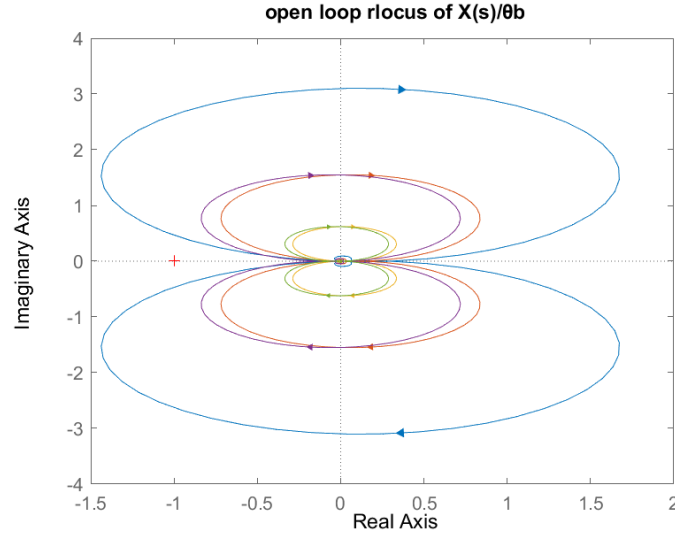


Figure 11: Nyquist contour of $\frac{X(s)}{\theta_b(s)}$ at $gain = \pm 0.2, \pm 0.5, 1$.

In Figure 11, the Nyquist contours of $\frac{X(s)}{\theta_b(s)}$ at the provided proportional gains, do not encircle the critical point. Due to the lack of Nyquist clockwise encirclement of the critical point and lack of open loop unstable poles, $\frac{X(s)}{\theta_b(s)}$ will not be unstable in a closed loop configuration, thus only a proportional gain would be required as the system is inherently stable.

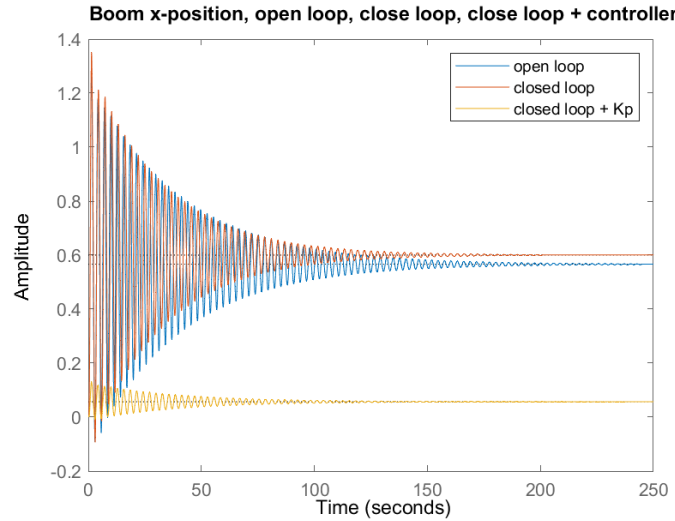


Figure 12: different step response of $\frac{X(s)}{\theta_b(s)}$.

To analyse the efficacy of $\frac{X(s)}{\theta_b(s)}$ in a closed loop configuration, a step input of -10 will be used to observe its step response as it simulates the initial x-location of the load. Furthermore, this system will be compared with its open loop configuration and its configuration with a proportional controller. A proportional gain controller of 0.1 has proven to be efficacious when reducing oscillating amplitude to fit within 0.2 m after 5 seconds condition. As a result, we can confirm that the controller used for $\frac{X(s)}{\theta_b(s)}$ in a feedback configuration to be $K_p = 0.1$ as shown in Figure 12.

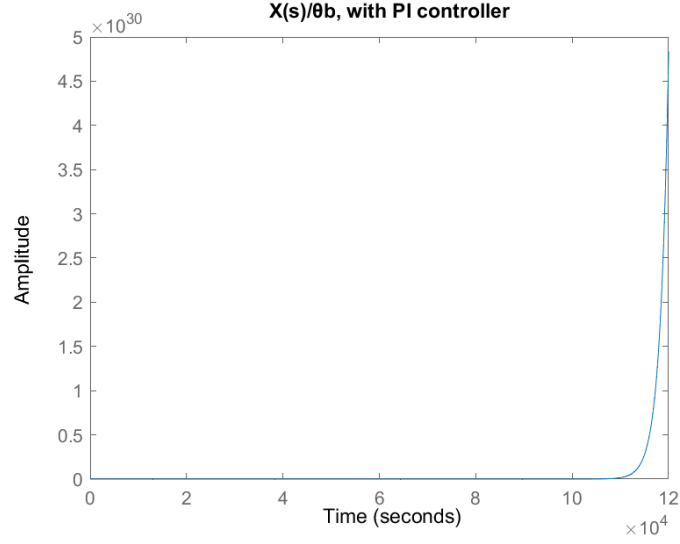


Figure 13: step response of $\frac{X(s)}{\theta_b(s)}$ with a PI.

When designing the controller for $\frac{X(s)}{\theta_b(s)}$, only the proportional control was required as introducing an integral controller will cause the system to be unstable as shown in Figure 13. This was expected as introducing a pole without a zero often leads to instability in a system. Thus, the controller transfer function for $\frac{X(s)}{\theta_b(s)}$ can be generated below.

$$C_{\frac{X(s)}{\theta_b(s)}}(s) = 0.1$$

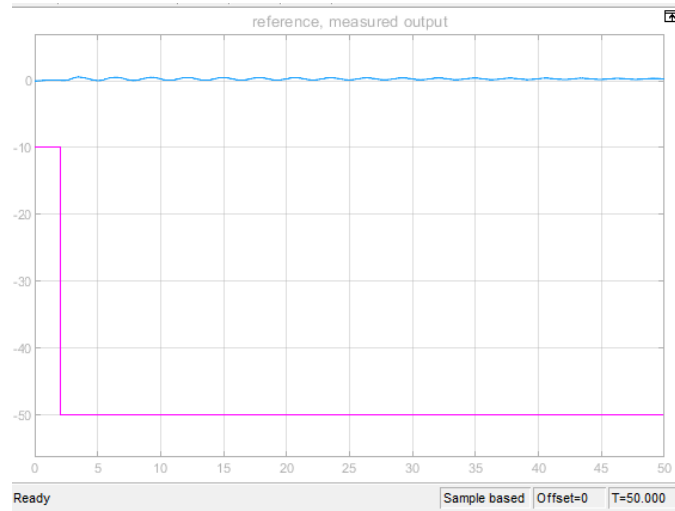


Figure 14: step response of $\frac{X(s)}{\theta_b(s)}$ with $K_p = 0.1$, in a simulated environment.

As illustrated in Figure 14, when $\frac{X(s)}{\theta_b(s)}$ was simulated in Simulink with a proportional controller of 0.1. the system oscillates within the conditions of ± 0.2 m complying with the objective.

X-controller produces motion in the y-direction of the load because of the motion of the boom.

As observed in Figure 15, when the boom receives a step input of -10, it produces motion in the y-direction of the load. This is because the boom controls both the x and y location of the load. Additionally, the closed loop configuration of $\frac{Y(s)}{\theta_b(s)}$ has shown to provide similar results as its open loop configuration, as gravity would help the load reach equilibrium in the event of a y-axis displacement from the boom.

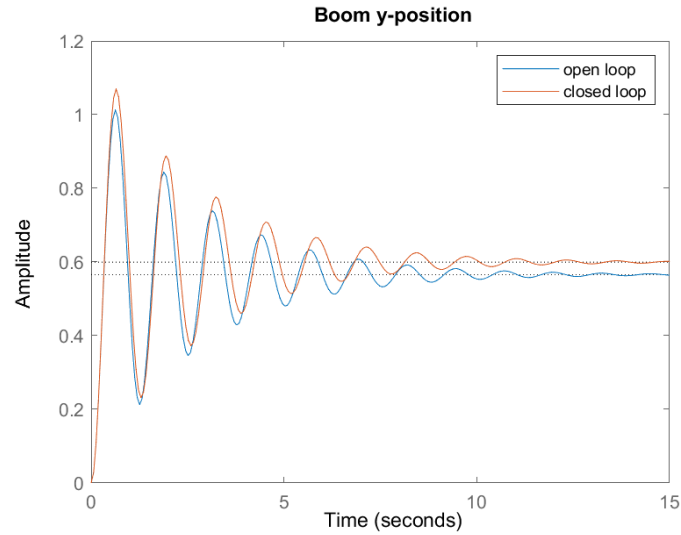


Figure 15: different step response of $\frac{Y(s)}{\theta_b(s)}$.

Although, the y-axis oscillation of the load cannot be controlled with a y-axis boom controller. Y-axis of the load can be dampened by designing controller for the winch $\frac{Y(s)}{\theta_w(s)}$.

Design a controller for the winch to control the y-position of the load.

To dampen the y-direction of the load, a controller unit must be introduced to the winch. When designing a controller unit for this system, a comparison between its open loop, closed loop, closed loop with proportional controller, and closed loop with proportional integral controller was observed for its stability, when provided with a step input as illustrated in Figure 16.

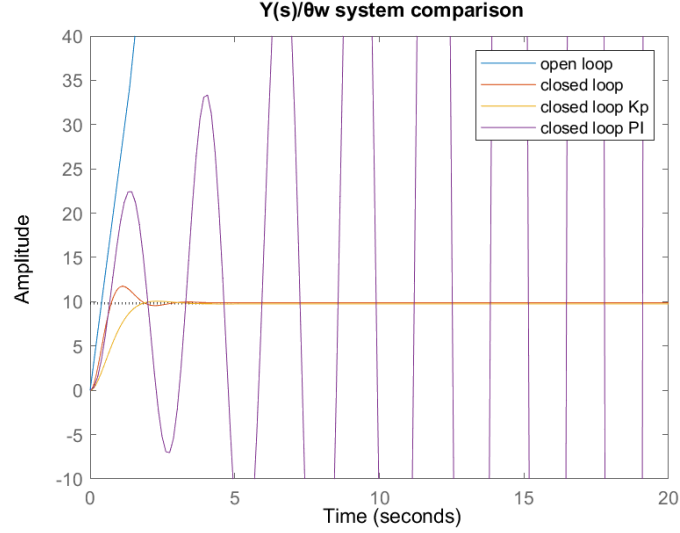


Figure 16: Step response of different $\frac{Y(s)}{\theta_b(s)}$ configurations.

Using only a closed loop feedback system, or a closed loop feedback system with a proportional controller of 0.4 was observed to be feasible; achieving a steady state within 5 seconds and having steady state errors of ± 0.1 m or ± 0.225 m respectively. In comparison to the PI controlled configuration which resulted in instability. However, when placed in Simulink, the step response of the Kp controller proved to be ineffective when provided with the same step input.

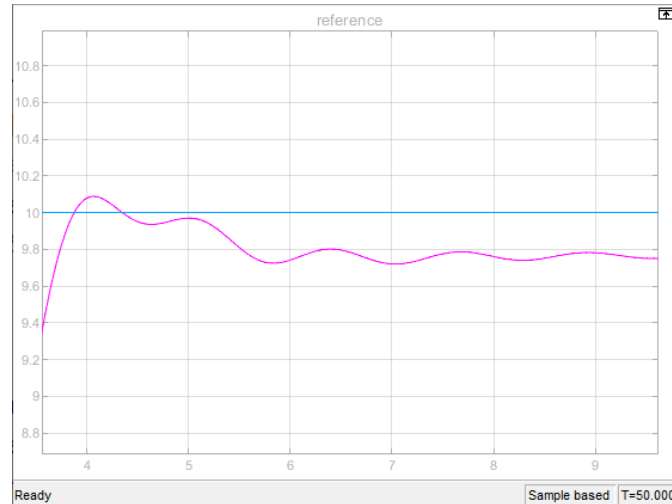


Figure 17: Step response $\frac{Y(s)}{\theta_w(s)}$ with $K_p = 0.4$ in a simulated environment.

As shown in Figure 17, when the closed loop winch system was placed in Simulink with $K_p = 0.4$, it would not achieve the expected steady state within 5 seconds; provided that the filter coefficient was 20. This is because in reality, controller that accepts a continuous time

input would need to be processed in discrete time, thus, factors such as filter coefficient should be considered.

To address the issue in Figure 17, Simulink offers an auto-tune option for the PID controller block. Hence, this auto-tune controller technique was leverage to minimise oscillation, overshoot, and improve the overall robustness of the system. This can be shown in Figure 18 where the oscillation is expected to change. However, this option requires original PID arguments inputs for the auto-tune to alter, which its original transfer function can be provided below.

$$C_{\frac{Y(s)}{\theta_{\omega}(s)}}(s) = 0.4 + \frac{2}{s} + 5 \frac{30}{1 + \frac{30}{s}}$$

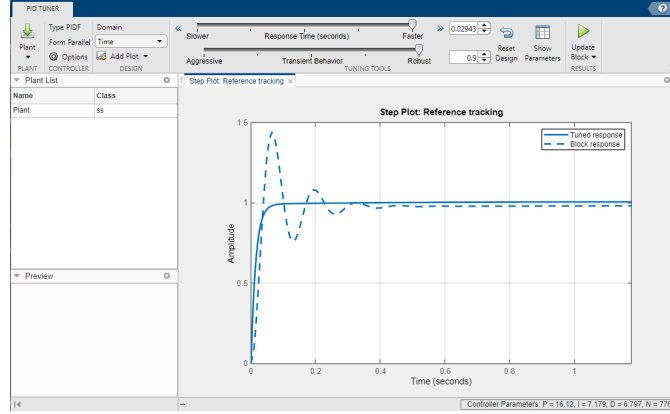


Figure 18: Expected auto-tuned result of $\frac{Y(s)}{\theta_{\omega}(s)}$ controller.

The PID controller that was generated by the auto-tune system, has addressed the final condition of the objective, ensuring that the y-axis does not oscillate more than ± 0.1 m, as illustrated in Figure 19. As a result, the transfer function of the $\frac{Y(s)}{\theta_{\omega}(s)}$ PID controller is generated below.

$$C_{\frac{Y(s)}{\theta_{\omega}(s)}}(s) = 16.1 + \frac{7.18}{s} + 6.80 \frac{7766}{1 + \frac{7766}{s}}$$

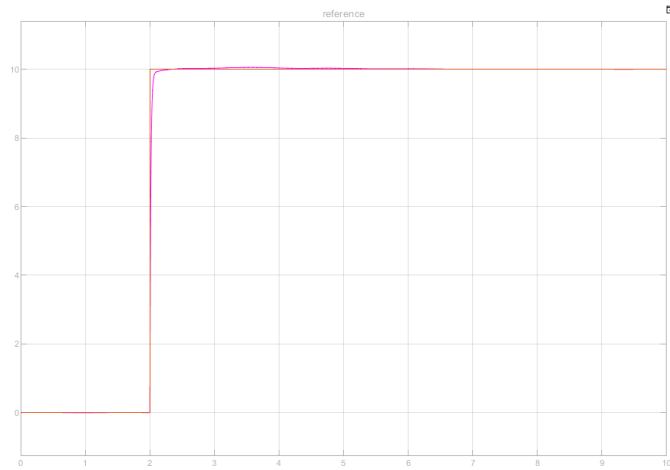


Figure 19: step response of $\frac{Y(s)}{\theta_{\omega}(s)}$ with an auto-tuned PID controller.

Finally, the entire system should be coupled together similarly to a general 2 input, 2 output manner as shown in Figure 20. This configuration considers only the relevant controllers $C_{\frac{Y(s)}{\theta_\omega(s)}}(s)$, $C_{\frac{X(s)}{\theta_b(s)}}(s)$ and the relevant systems stated in page 9.

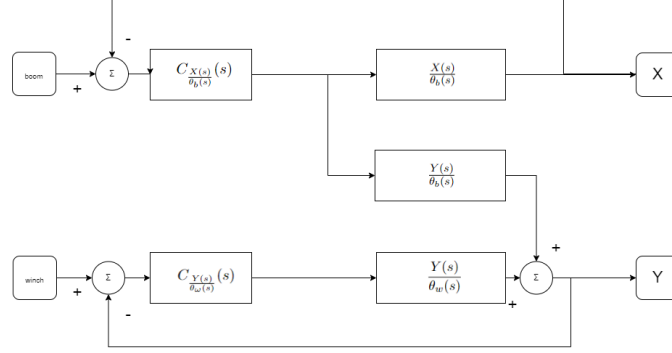


Figure 20: Feedback control for the 2 input, 2 output crane system

The final Simulink configuration for the crane can be observed in Figure 21. This configuration encompasses the controllers and the relevant boom and winch transfer functions.

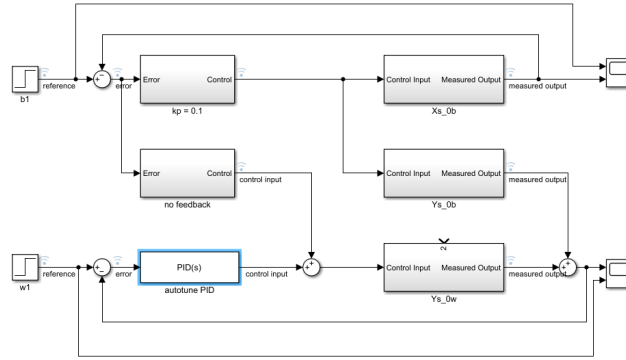


Figure 21: Feedback control for the 2 input, 2 output crane system in Simulink.

Finally, the overall output of the system can be seen in Figure 22, where the magenta line represents the step input. This complies with the condition of having $\theta_b = -10$ (which we intend to remove), whilst oscillating less than 0.2 m in the x-axis direction. Furthermore, when given a step input of $\theta_\omega = 10$, the y-axis is dampened according using the auto-tuned PID controller, whilst maintaining a less than 0.1 m oscillation in the y-axis.

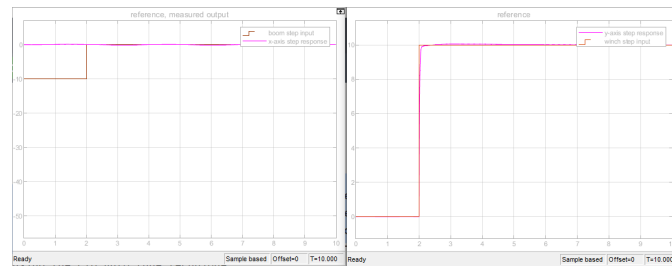


Figure 22: Crane output in the x-axis(left) and y-axis(right) when given a boom/winch displacement input